Computational Toxicology 26 (2023) 100264

Contents lists available at ScienceDirect

Computational Toxicology

journal homepage: www.sciencedirect.com/journal/computational-toxicology

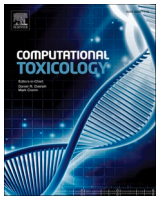

Computational perspectives on Chlorpyrifos and its degradants as human glutathione S-transferases inhibitors: DFT calculations, molecular docking study and MD simulations

Nikita Tiwari [a], Anil Mishra [b,*]

[a] Department of Chemistry, Shri Ramswaroop Memorial College of Engineering & Management, Lucknow, Uttar Pradesh 226010, India
[b] Department of Chemistry, University of Lucknow, Lucknow 226007, India

ARTICLE INFO

Keywords:
Chlorpyrifos
DFT
Basis set
Docking
Simulation
Glutathione S-transferases

ABSTRACT

Chlorpyrifos is the toxicant chemical from the class of organophosphorus insecticides. The insecticide undergoes environmental degradation to chlorpyrifos-oxon (CPYO), des-ethyl chlorpyrifos (DEC), 3,5,6-trichloro-2-methoxypyridine (TMP) and 3,5,6-trichloro-2-pyridinol (TCP). Herein, CPF along with its degradants were optimized employing density functional theory (DFT) and B3LYP/6-311G+(d,p) basis set to elucidate their thermal and frontier molecular orbital properties. The DFT outcome revealed that TCP showed the lowest HOMO-LUMO gap (4.38 eV), also highest dipole moment, electrophilicity index and basicity. Docking was done using AutoDock 4.2.6 against human glutathione S-transferases to search binding affinity and interactions of all pollutants with the protein. The docking results expressed that TCP required least binding energy (−5.51 kcal mol^{-1}) which is relatable to the DFT studies and might act as the most powerful inhibitor. GROMACS 5.1.1 was utilized to perform simulation studies for each ligand–protein docked complexes. Results concluded that CPF, DEC, TMP, CPYO and TCP could possibly perform as toxic and inhibit enzymatic activity by interrupting the metabolic pathways in humans.

1. Introduction

Chlorpyrifos belongs to an organophosphorus class of pesticide that is most broadly used for pests control [1]. This chemical can inhibit several proteins like acetylcholinesterase, glutathione S-transferases (GSTs) and many others [2]. Chlorpyrifos (CPF; *O*,*O*-diethyl-*O*-3,5,6-trichloro-2-pyridylphosphorothioate) is an insecticide from organophosphorus class and researchers reported it as an endocrine disruptive chemical (EDC) [3]. The main pathway of CPF involves its degradation into various intermediates (Racke, K. D., 1993) as shown in Fig. 1, such as Chlorpyrifos-oxon (CPYO), 3,5,6 Trichloro-2-methoxypyridine (TMP) and Des-ethyl Chlorpyrifos (DEC), 3,5,6- Trichloro-2-pyridinol (TCP), which can disturb the endocrine system. The main metabolites of this toxic substance are TCP and DEC. By cytochrome P450-mediated oxidative desulfuration in human beings, chlorpyrifos gets activated in the form of toxic oxygen analogs [4,5]. CPYO (oxon) inhibits acetycholinesterase activity but it hydrolyzes much more rapidly than CPF. Its detoxification involves conjugation of oxon with glutathione, catalyzed by Glutathione S-transferase [6]. GST has many properties including antioxidant along with anti-inflammatory properties as it metabolizes toxicants like carcinogens. Pesticides resistance is also due to the participation of GSTs in organophoshorus pesticides (OPs) detoxification [7]. This enzyme is an essential part of the guarding mechanism against harmful chemicals. This also reduces cellular damage produced via chemical agents. However, the regulation and induction of GST due to organophosphates such as CPF and its degradants have not been reported yet.

Here, we target GSTs, a broad family of enzymes (detoxifying) present in many forms of life. Toxic effects of these OPs get inactivated by GSTs as it makes them soluble by chemically conjugating these toxicants to the glutathione and hence, these chemicals can be easily excreted out of the body. Pathogenic parasites are able to inactivate these drugs as they also make their own GSTs [8]. Organophopshorus pesticides resistance is directly correlated with the metabolism of these toxicants by GSTs. Glutathione S-transferases also contribute in resistance and this has been stated by many researchers that insects which show insecticide resistance have high levels of GSTs activity [9]. GSTs show an important role in many activities like hormones biosynthesis, intracellular

* Corresponding author.
E-mail address: mishraanil101@hotmail.com (A. Mishra).

https://doi.org/10.1016/j.comtox.2023.100264
Received 1 July 2022; Received in revised form 27 February 2023; Accepted 27 February 2023
Available online 3 March 2023

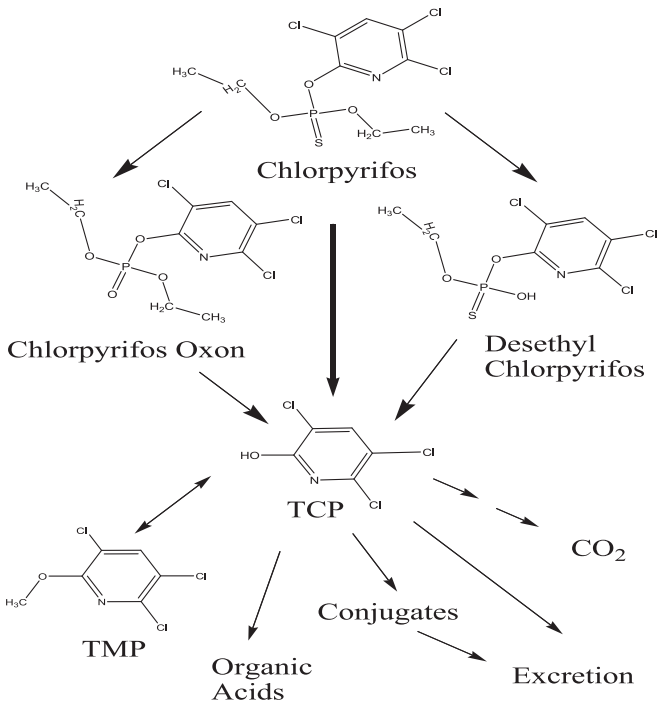

Fig. 1. Generalized pathways of chlorpyrifos transformation in the environment.

transport and it also provides oxidative stress protection. Free radicals produced majorly by the insecticidal action are toxic oxygen species and are removed by GSTs. Also, they show peroxidase [10] and isomerase activity [11], which inhibits the junction of N-terminal kinase and it is capable of binding to a wide range of ligands, non-catalytically [12].

Animal testing has been reduced and replaced by the recent trend that led to several in silico methods for understanding toxicity [13]. Quantum mechanical techniques such as density functional theory (DFT) can be used to compute and create descriptors for use in predictive toxicity models [14]. Descriptors based on DFT are very useful in predicting atomic and molecular reactivity [15]. The usefulness of the electrophilic index in elucidating the toxicity of polychlorinated biphenyls [16] and benzidine [17] was analysed in many research. The power of DFT method in describing structural, energetic and magnetic molecular properties is well established [18]. Within the framework of conceptual density functional theory, several global and local reactivity parameters are available that serve as effective descriptors for predicting biological and toxicological activity [19]. A recent study used HOMO-LUMO energy gap derived from DFT as a descriptor to predict Ames mutagenicity data for aromatic primary amines [20]. It is important to note that computational methods such as DFT calculations and molecular mechanics (docking and molecular dynamics) have the advantage of being able to reproduce experimental data while saving computational time and memory [21].

The present in silico study has been performed to verify that chlorpyrifos along with its degradants binding to glutathione S-transferases is energetically possible or not. The aim of the present work involved computational perspectives to understand overall molecular interactions of chlorpyrifos along with its degradants (CPYO, DEC, TMP and TCP) with glutathione S-transferases using DFT calculations, docking and MD simulation studies. Docking studies provides the prediction for a possible molecular interaction of toxic compounds with enzymes of many important pathways leading to the production of vital molecules [22].

2. Methods and materials

An approach has been used to find the human glutathione S-transferases protein target for Chlorpyrifos and its degradants. This includes optimization of compounds which was carried out at the B3LYP/6-311 + G(d,p) level of theory, implemented in the Gaussian 09 W package of programs and molecular docking which was performed using AutoDock 4.2.6 for target protein–ligand complex. Finally to observe the stability of protein–ligand complex, simulation study was undertaken employing Gromacs 5.1.1 suite.

2.1. Quantum chemical calculations

These calculations were undertaken employing DFT with B3LYP method using 6-311 + G (d,p) basis set employing Gaussian 09W [23]. The 3-D structures of compounds Chlorpyrifos and its degradants were optimized. The molecular structures for the selected ligands were drawn by GaussView 5.0 [24], as pictured (Fig. 2). Vibration analysis showed no negative eigenvalues, indicating a minimum on Potential Energy Surface. For every molecule's free energy, polarization, also the dipole was calculated. The molecular orbitals known as HOMO & LUMO, the Molecular Electrostatic Potential, and the Mulliken charges evaluations were performed employing the same basis sets. The mathematical details (equations) utilized for the determination of global properties have been reported earlier [25,26]. According to Koopmans' approximation [27], ionization potential & electron affinity were expressed in terms of the HOMO and the LUMO as:

Ionization Potential (IP) = $-E_{HOMO}$.

Electron Affinity (EA) = $-E_{LUMO}$.

Pearson [28] introduced chemical hardness, a quantum chemical parameter to explain the stability of given compound as,

$$\text{Chemical Hardness}\,(\eta) = \frac{1}{2}(\text{IP} - \text{EA})$$

The given equations were utilized for the evaluations of other parameters like electrophilicity index (ω), softness (δ) and electronegativity (χ):

$$\chi = -\frac{1}{2}\,(\text{EHOMO} + \text{ELUMO})$$

$$\delta = 1/\eta$$

$$\omega = \chi^2/2\eta$$

2.2. Protein preparation and molecular docking

Computational docking was employed to assess the binding patterns of the chlorpyrifos (also its degradants) with human glutathione S-transferases. The three-dimensional structure of human glutathione S-transferases (PDB ID: 4GTU) was retrieved as PDB format file from the RCSB database [29]. The optimized compounds were then utilized for docking study against human glutathione S-transferase (GST).

AutoDock 4.2.6 was employed to perform the docking process for Chlorpyrifos along with its degradants with human glutathione S-transferases [30]. Autodock uses a semi-empirical force field to verify the binding affinity of the selected ligands to a macromolecule. Receptor molecule was prepared by adding explicit hydrogen molecules and associated Kollman charges (16.0) by utilizing the AutoDock Tools 1.5.6 and saved in.pdbqt file format. Chlorpyrifos (CPF; *O*,*O*-diethyl-*O*-3,5,6-trichloro-2-pyridylphosphorothioate) including its degradants chlorpyrifos-oxon (CPYO), des-ethyl chlorpyrifos (DEC), 3,5,6 trichloro-2-methoxypyridine (TMP) and 3,5,6- trichloro-2-pyridinol (TCP) were used for docking studies with human glutathione S-transferases. The 3-D molecular structures of all the chemicals were drawn using GaussView5 and minimized using Gaussian09 software. Hydrogen atoms and Gasteiger charges were added while preparing the ligands and then finally

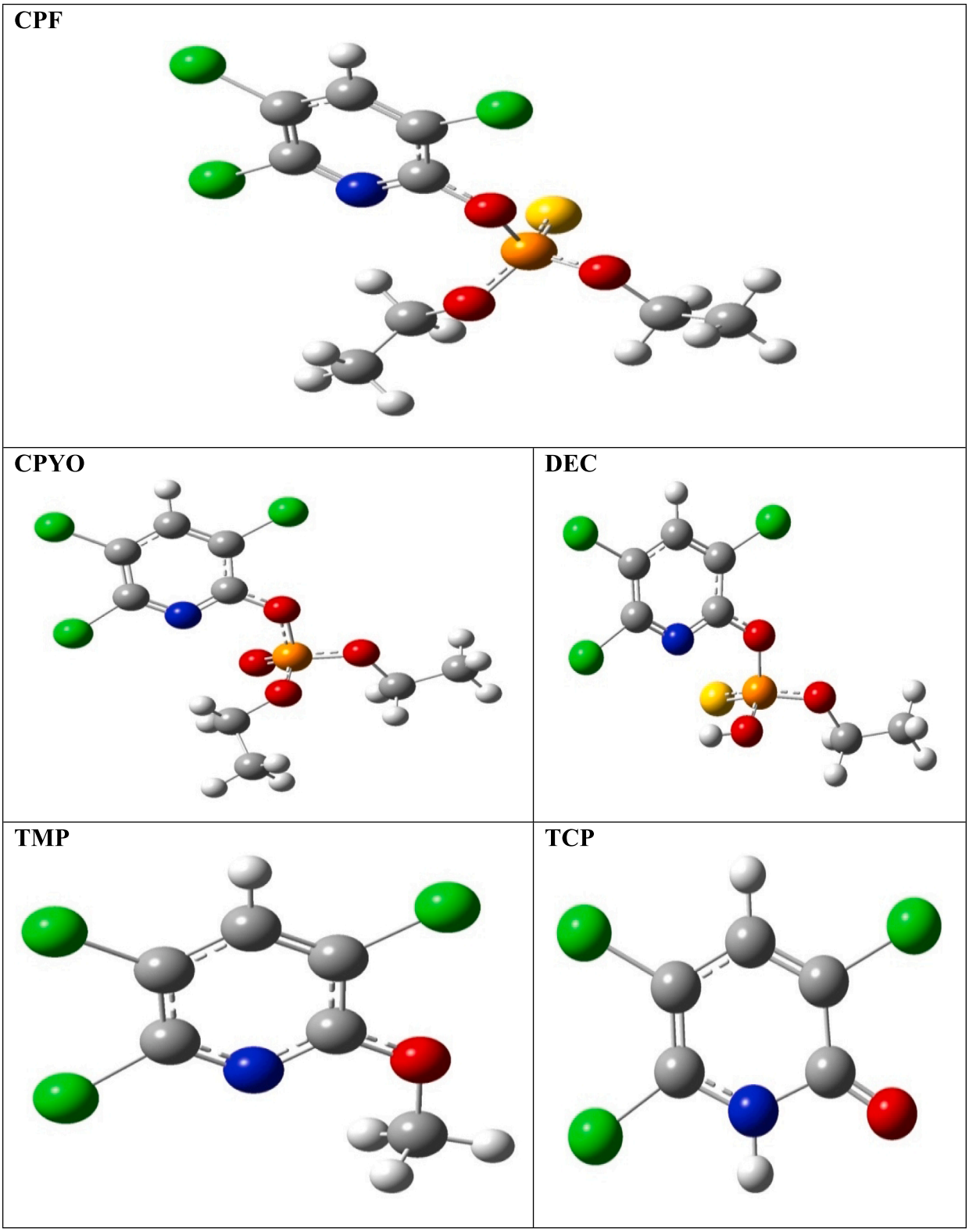

Fig. 2. Optimized geometrical structures of the five ligands, i.e., CPF, CPYO, DEC, TMP and TCP. CPF, chlorpyrifos; CYPO, chlorpyrifos-oxon; DEC, des-ethyl chlorpyrifos; TCP, 3,5,6-trichloro-2-pyridinol; TMP, 3,5,6-trichloro-2-methoxypyridine.

saved in.pdbqt format. To specify the torsional degrees in ligand molecule, ligand flexibility was utilized. For docking purpose, Lamarckian Genetic Algorithm method was adopted. The other remaining parameters for docking were taken as default. The pose with the maximum binding affinity and its respective interactions were selected and further visualized and analyzed in PyMol 1.3 [31].

2.3. Molecular dynamics simulation

The associated internal motion and dynamic process occurring at the

Table 1
Selected thermodynamic parameters of Chlorpyrifos (CPF) and its degradants (CPYO, DEC, TMP and TCP).

Name	Free energy (Hartree)	Dipole moment (Debye)	Polarization (Bohr^3)
CPF	−2743.286	2.81	184.20
CPYO	−2420.649	2.43	165.97
DEC	−2665.208	2.47	162.19
TMP	−1741.779	1.31	121.99
TCP	−1702.464	3.09	108.95

atomic level in GST on the binding of chlorpyrifos and its degradants were evaluated by molecular dynamics simulation. The simulation study was undertaken employing Gromacs 5.1.1 suite with GROMOS96 43a1 force field [32,33] and the periodic boundary conditions. The topology files were generated using Prodrug server for all the five investigated organophosphates. In a box (cubic), the protein–ligand complexes solvation was done applying simple point charges water molecules. For the neutrality, addition of oppositely charged ions was undertaken. Further, energy was minimized to reduce steric disturbances utilizing an algorithm (steepest descent). Thereafter, the equilibration of the given system was conducted with constant particles, volume, temperature, i.e., NVT for 50,000 steps, each step 2 fs. Again the equilibration was performed with constant particles, pressure, temperature, i.e., NPT (the ensemble at 300 K). The simulation was finally conducted for 20 ns, each step for 2 fs. The analysis of the saved trajectories was performed via Qtgrace. Root mean square deviation or RMSD, gyration, hydrogen bond numbers, root mean square fluctuation or RMSF, along with total solvent accessible surface area (SASA) were determined utilizing the tools of GROMACS, i.e., g rms, g rmsf, g gyrate, gmx sasa and g hbond tools, respectively.

3. Results and discussion

3.1. DFT calculations studies

The computational calculations for all the ligands were undertaken using the Gaussian 09 W package. The compounds were first designed on GaussView 5.0.9 then by using the Gaussian calculation setup, the geometries of all the compounds have been optimized at DFT 6-311G+(d, p) basis set at gas phase, pictured in Fig. 2. Vibrational frequencies at the ground state were determined to ensure that they were at the minimum level.

3.1.1. Thermodynamic properties

The stability conformation of the product obtained from any reaction and also spontaneity of any reaction is predicted from its thermodynamic properties like free energy. Greater negative value indicates improved thermodynamic properties. During this work, the values for free energy was found to be negative depicted in Table 1 explains that a reaction will occur spontaneously with none extra energy expense.

The DFT estimated data revealed that the moment of CPF is 2.81 Debye whereas TCP shows the very best dipole moment (3.09 Debye). High level of dipole moment accelerates the chemical bond formation, non-bonding interaction, binding affinity, including polar nature of a molecule. The polarizability of any given molecule is mainly dependent on the complexity of its structure and also on how the electron cloud be laid low with incoming charge. Large sized molecules are therefore, more polarizable. It's worth noting that the TCP is the smallest in size and has the smallest amount polarizability (108.95 Bohr^3), however, CPF has the highest complex structure and is predicted to own the highest polarizability, 184.20 Bohr^3.

The estimated DFT calculations for thermal parameters, dipole moment and also the polarizability values for chlorpyrifos (CPF) along

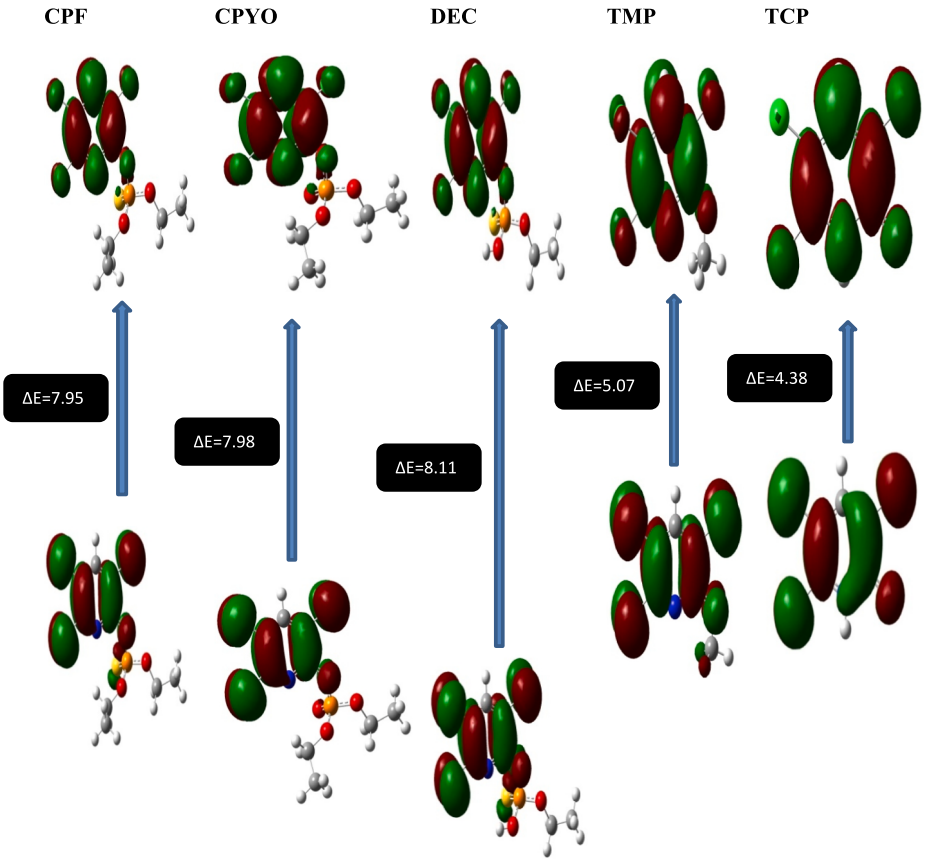

Fig. 3. Frontier molecular orbital (HOMO-LUMO) and related transition energy of Chlorpyrifos (CPF) and its Degradants (CPYO, DEC, TMP and TCP).

Table 2
HOMO, LUMO, Gap, hardness (η), electronegativity (χ), softness (δ), electrophilicity index (ω), ionization potential (IP) and electron affinity (EA) of all compounds.

Name	HOMO	LUMO	Gap	η	χ	δ	ω	IP	EA
CPF	−9.47	−1.52	7.95	3.97	5.49	0.25	3.79	9.47	1.52
CPYO	−9.54	−1.56	7.98	3.99	5.55	0.25	3.85	9.54	1.56
DEC	−9.57	−1.46	8.11	4.05	5.51	0.24	3.74	9.57	1.46
TMP	−6.84	−1.77	5.07	2.53	4.30	0.39	3.65	6.84	1.77
TCP	−6.73	−2.35	4.38	2.19	4.54	0.45	4.70	6.73	2.35

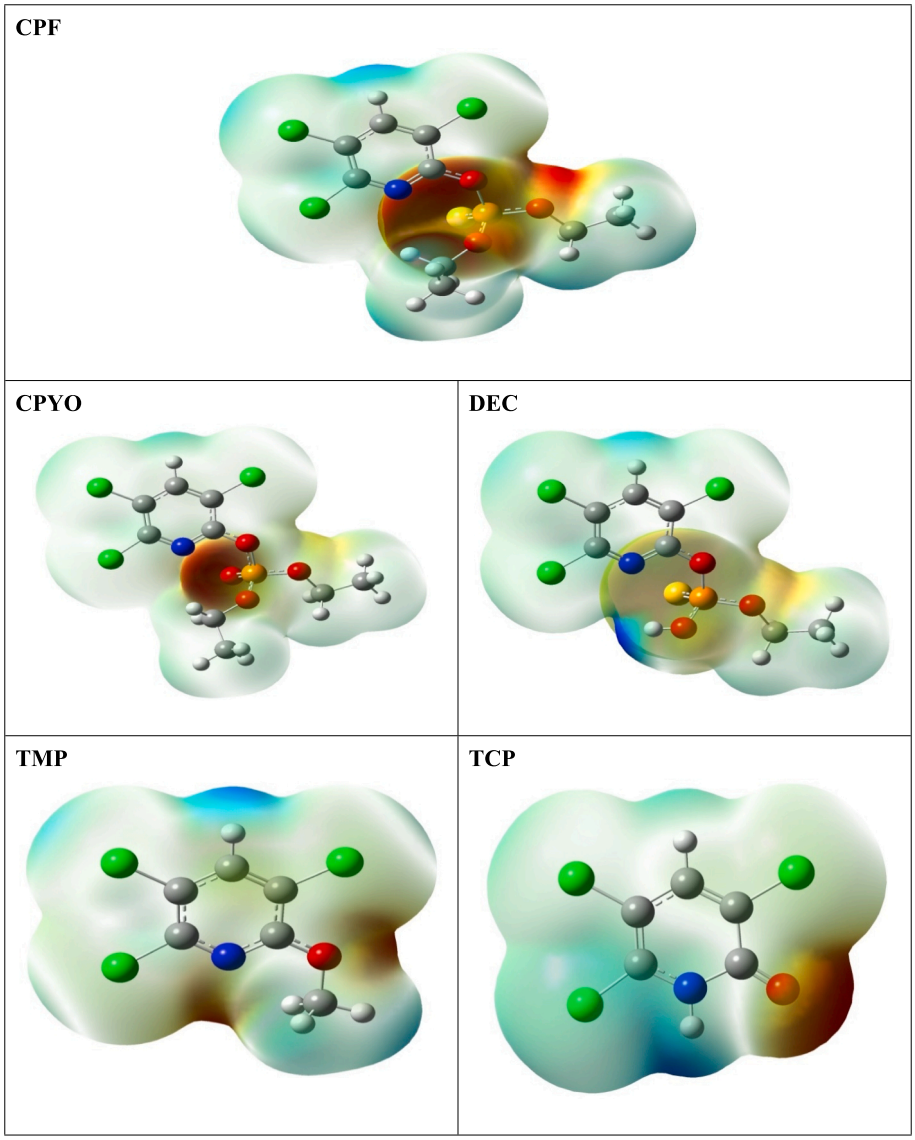

Fig. 4. Molecular electrostatic potentials (MEP) of compounds (CPF, CPYO, DEC, TMP and TCP).

with its degradants (CPYO, DEC, TMP and TCP) are summarized in Table 1.

3.1.2. Molecular orbital properties

The regions of space that contain the electron density are the molecular orbitals. These orbitals are defined by mathematical functions that explain the wave behaviour of the electrons. These functions can be further used to evaluate properties (chemical and physical) like an electron finding probability in a region of space.

HOMO- LUMO gap (ΔE) is used to evaluate chemical hardness of a compound and also the softness. High kinetic stability and low chemical reactivity is due to the large HOMO-LUMO gap and low HOMO-LUMO gap is related to less chemical stability, because in a given reaction, increment of electrons into a LUMO (high-lying) or withdrawal of electrons from a HOMO (low-lying) is energetically feasible. The molecular orbitals for investigated compounds are pictured in Fig. 3.

In this study, CPF shows the HOMO-LUMO gap to be 7.95 eV whereas TCP shows the lowest energy gap (4.38 eV) along with the highest chemical softness (0.45 eV) & electrophilicity index (4.70 eV) values which may contribute towards the higher chemical reactivity than other degradants (Table 2).

3.1.3. Molecular electrostatic potential (MEP)

To verify the reactive nature of any given compound, the molecular

Table 3
The Mulliken atomic charges of the estimated compounds (CPF, CPYO, DEC, TMP and TCP).

CPF		CPYO		DEC		TMP		TCP	
1C	−1.602496	1C	−2.087050	1C	−1.379657	1C	−0.571596	1C	−1.005233
2C	1.368406	2C	1.750181	2C	1.226449	2C	0.552703	2C	0.640896
3C	−1.300734	3C	−1.252228	3C	−1.286228	3C	−1.560865	3C	−1.213709
4C	0.630252	4C	0.624242	4C	0.486203	4C	1.497918	4C	0.442277
5C	−0.461272	5C	−0.400667	5C	−0.341524	5C	−1.530411	5C	−0.064543
6 N	0.187295	6 N	0.147956	6 N	0.092669	6 N	0.094837	6 N	0.216489
8Cl	0.311266	8Cl	0.320375	8Cl	0.298950	8Cl	0.506545	8Cl	0.446765
9Cl	0.406003	9Cl	0.404561	9Cl	0.418559	9Cl	0.481075	9Cl	0.462548
10Cl	0.240177	10Cl	0.233311	10Cl	0.224168	10Cl	0.345480	10Cl	0.377937
11O	−0.030927	11O	−0.144331	11O	−0.089508	11O	−0.107869	11O	−0.303428
12P	0.501081	12P	0.770787	12P	0.693269	12C	0.292183		
13O	−0.026250	13O	−0.142416	13O	−0.080917				
14O	−0.142969	14O	−0.234828	14O	0.025723				
15C	0.192393	15C	0.269033	15 S	−0.378327				
16C	0.023622	16C	−0.151751	16C	0.103353				
22 S	−0.314669	22C	0.175511	17C	−0.013183				
23C	0.094989	23C	−0.043778						
24C	−0.076168	29O	−0.238909						

electrostatic potential is a key aspect to be determined. It gives a picture for the molecular shape and size of negative, positive, also the neutral potential. MEP proved to be an important tool for the prediction of relationship between physicochemical property and molecular structure of compounds under investigation. Moreover, this may be utilized to evaluate the reactivity of compounds toward different attacks (electrophilic and nucleophilic). The MEP for the investigated compounds is deliberated using the same basis sets as illustrated in Fig. 4.

This potential plot shows that the electrophilic attack is preferred at maximum negatively charged locations which are indicated with red colour. Thus, this region will attract an attacking electrophile, and the opposite will happen for the regions indicated with blue. The molecular shape, the size and orientation of the neutral, positive, and the negative electrostatic potential differ molecule to molecule due to type of atoms including its electronic nature. The variation for the interaction with the receptor is therefore, due to the variation in the MEP of the compounds.

3.1.4. Mulliken atomic charges

The atomic charges of the estimated compounds were determined with the DFT using B3LYP 6 as a method at −311G+ (d, p) basis set and these calculations are tabulated in Table 3. The obtained results found that C2 is bearing highly positive and C1 is bearing highly negative charge for CPF. Also, it is observed that the most nucleophilic centres of CPYO are C1 and C3, the most electrophilic susceptibility positions. From the results, it is obvious that the susceptibility towards nucleophile of CPYO is recognized on C2 and P12 sites. However, C1 and C3 are highly negative charges of DEC, TMP and TCP and their respective positively charged atoms are C2, C4 and C2**.** The nucleophiles attack at positively charged centres and for electrophilic attacks, the most susceptible site is negatively charged centres.

3.2. Binding affinity and binding interactions analysis

The docking study is a most widely used computational approach to ensure the binding of the suitable orientation of ligand with the target macromolecule. The molecular interactions were characterized by performing docking studies for chlorpyrifos, along with its degradants within active site cavity of the human glutathione S-transferases using AutoDock 4.2.6. The binding energies of the toxicants were compared to some known inhibitors of GST such as coumarin (-4.62 kcal/mol) and citric acid (−3.04 kcal/mol) and thus these are considered as strong inhibitor candidates [34]. All the generated binding poses were ranked on their binding affinities, accordingly and the AutoDock outcome illustrated that Chlorpyrifos (CPF) showed a binding energy of −5.04 kcal/mol whereas increasing order of binding energy of the degradants followed the sequence such as CPYO < DEC < TMP < TCP (−4.37 < −4.97 < −5.48 < −5.51) kcal/mol, shown in Table 4.

The docking of CPF with GST showed that CPF packed against 16 human glutathione S-transferases residues (Tyr-6, Ile-9, Gly-11, Leu-12, Arg-42, Asn-58, Leu-59, Pro-60, Ser-107, Asn-108, Ala-111, Leu-165,

Table 4
Binding energy values, types of interactions, number of bonds and common interacting residues of CPF, CPYO, DEC, TMP and TCP, which were evaluated using rigid docking with human glutathione S-transferases.

Ligands	Binding energy (kcal/mol)	Type of interactions		Number of bonds		Common residues
		H-bond residues	Hydrophobic bond residues	H-bonds	Hydrophobic bonds	
CPF	−5.04	Tyr115 (3.2 Å, 3.6 Å)	Tyr6, Ile9, Gly11, Leu12, Arg42, Asn58, Leu59, Pro60, Ser107, Asn108, Ala111, Leu165, Leu207, Tyr208, Thr209	2	15	Tyr6 Ile9 Gly11 Leu12 Asn108 Ala111 Tyr115 Leu207 Tyr208 Thr209
CPYO	−4.37	Tyr6 (3.2 Å), Tyr115 (3.0 Å)	Trp7, Ile9, Arg10, Gly11, Leu12, Asn58, Leu59, Pro60, Asn108, Ala111, Leu207, Tyr208, Thr209	2	13	
DEC	−4.97	Tyr6 (2.8 Å, 3.0 Å)	Trp7, Ile9, Gly11, Leu12, Asn58, Leu59, Pro60, Asn108, Ala111, Tyr115, Leu207, Tyr208, Thr209	2	13	
TMP	−5.48	–	Tyr6, Ile9, Arg10, Gly11, Leu12, Ser107, Asn108, Leu110, Ala111, Tyr115, Asp161, Leu165, Leu207, Tyr208, Thr209	0	15	
TCP	−5.51	Tyr6 (3.5 Å), Tyr208 (2.0 Å), Thr209 (3.1 Å)	Ile9, Arg10, Gly11, Leu12, Ser107, Asn108, Ala111, Tyr115, Leu165, Leu207	3	10	

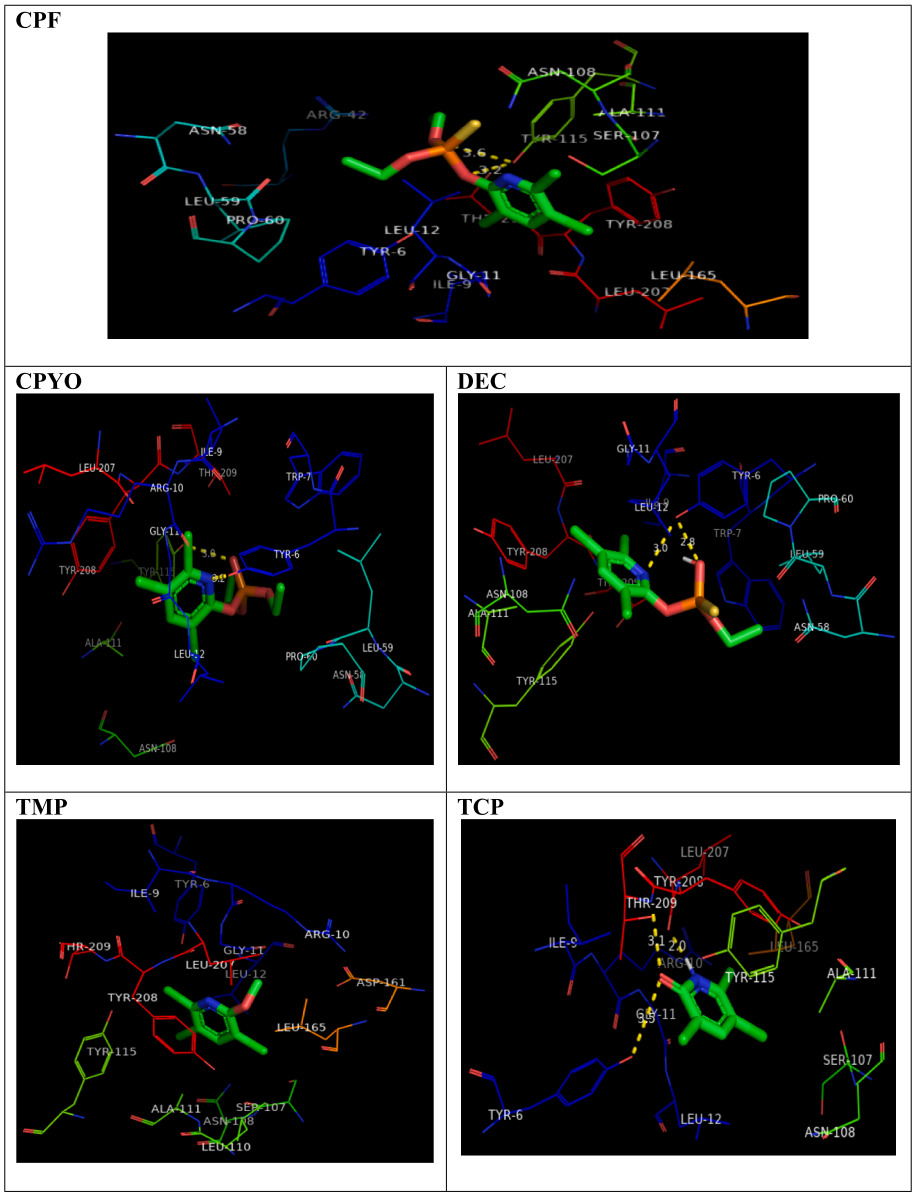

Fig. 5. Amino acid residues in the binding pocket of human glutathione S-transferases involved in interactions with the following: CPF, CPYO, DEC, TMP, TCP. CPF, chlorpyrifos; CYPO, chlorpyrifosoxon; DEC, des-ethyl chlorpyrifos; TCP, 3,5,6- trichloro-2-pyridinol; TMP, 3,5,6-trichloro-2- methoxypyridine (yellow dots represent H-bond). (For interpretation of the references to colour in this figure legend, the reader is referred to the web version of this article.)

Leu-207, Tyr-208 and Thr-209). The OH moiety of the residue Tyr-115 formed two H-bonds with the oxygen atoms of the phosphate group of CPF. Except ordinary hydrogen bonding, nonbonding interactions are frequently used term to determine the shape and behaviour of molecules. The docking of CPYO with GST showed that CPYO binds with Tyr-6, Trp-7, Ile-9, Arg-10, Gly-11, Leu-12, Asn-58, Leu-59, Pro-60, Asn-108, Ala-111, Tyr-115, Leu-207, Tyr-208 and Thr209 residues within the active site of the macromolecule. The CPYO formed H-bonds with OH moiety of Tyr-6 and Tyr-115 residues. The evaluation of docking outcome clarify that the residue Trp-7, Ile-9, Gly-11, Leu-12, Asn-58, Leu-59, Pro-60, Asn-108, Ala-111, Tyr-115, Leu-207, Tyr-208 and Thr-209 interacted hydrophobically with the DEC molecule, also one H-bond (Tyr-6). However, TMP interacts hydrophobically with Tyr-6, Ile-9, Arg-10, Gly-11, Leu-12, Ser-107, Asn-108, Leu-110, Ala-111, Tyr-115, Asp-161, Leu-165, Leu-207, Tyr-208 and Thr-209 residues. The docking complex showed that TCP interacted with 13 GST residues (Ile9, Arg10, Gly11, Leu12, Ser107, Asn108, Ala111, Tyr115, Leu165, Leu207) within the active site of human glutathione S-transferases. The TCP formed hydrogen bonds against the residue, Tyr-6, Tyr-208 and Tyr-209 of the protein. Significant hydrogen bonding in CPF, CPYO, DEC and TCP not only contributes in increasing binding affinity but also increase binding specialty.

From molecular docking analysis, the major and common residues of glutathione S-transferases active site like Tyr6, Ile9, Gly11, Leu12, Asn108, Ala111, Tyr115, Leu207, Tyr208 and Thr209 form different significant interactions with the ligands, shown in Fig. 5. The evaluation of results concludes that all the compounds can effectively bind to the active site of human glutathione S-transferases. Moreover, TCP showed maximum binding affinity (-5.51 kcal/mol) in comparison to its parent compound, i.e., chlorpyrifos (-5.04 kcal/mol) and hence, can be the most potent inhibitor for this protein. In this work, analysis of molecular docking results may be helpful in the assessment of health problems produced by this organophosphorus pesticide. As the consumption of Chlorpyrifos is becoming more widespread, the potential risks may increase and more studies with detailed molecular mechanisms supported by in vitro studies are required to confirm the alteration of the

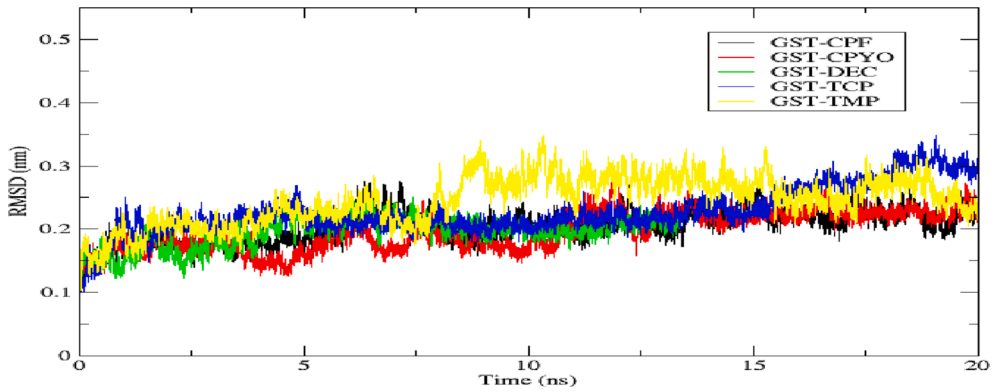

Fig. 6. RMSD profile of the Cα backbone of human glutathione S-transferases (GST) during the 20 ns of simulation at 300 K with chlorpyrifos (CPF) and its degradants (CYPO, chlorpyrifosoxon; DEC, des-ethyl chlorpyrifos; TCP, 3,5,6- trichloro-2-pyridinol; TMP, 3,5,6-trichloro-2- methoxypyridine).

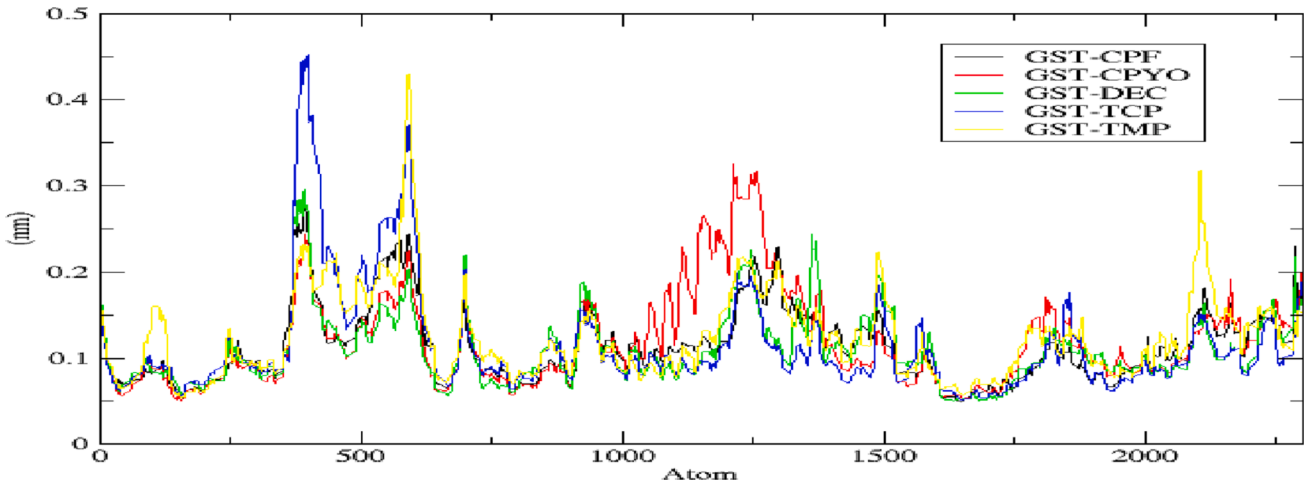

Fig. 7. RMSF molecular dynamics simulation results of human glutathione S-transferases (GST) for 20 ns with CPF and its degradants (CPYO, DEC, TCP and TMP).

metabolism pathway for the inhibiting mechanism of chloryrifos and its degradants in the human body.

3.3. Molecular simulation results

During the MD simulation, RMSD estimates the dynamic stability of the protein–ligand complexes and predicts the conformation changes occurring in the protein. In this current study, RMSD values for the investigated complexes were analyzed. RMSD graphs depicts that majority of the investigated system attains equilibrium near about 8 ns and were stable around 20 ns during the simulation (Fig. 6). The high fluctuation in RMSD values for the complexes lies within 2 Å to 3 Å. The

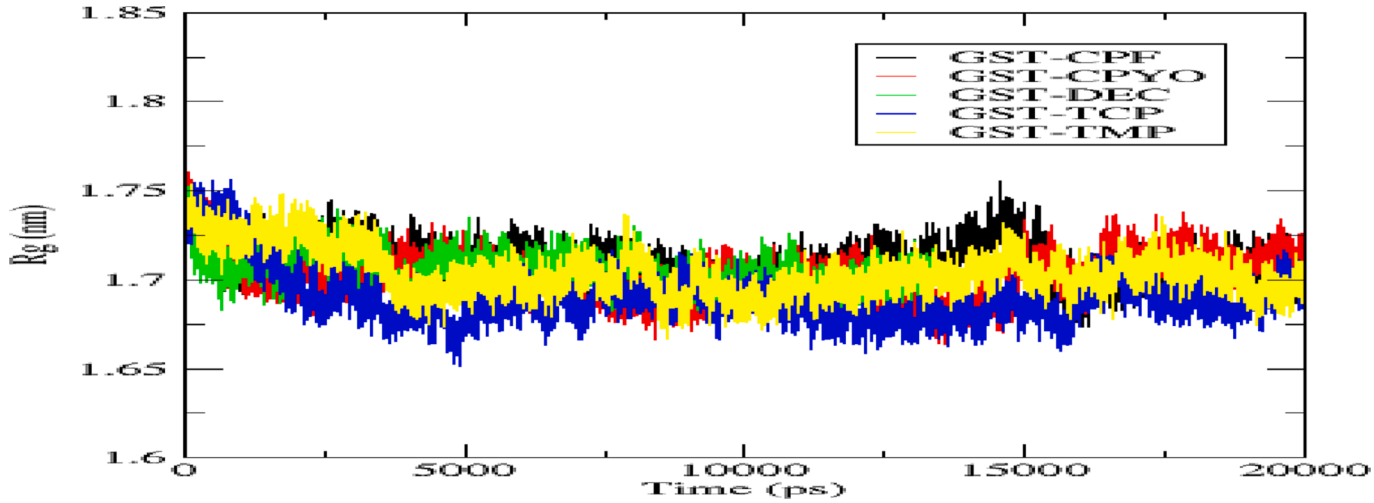

Fig. 8. Radius of gyration (Rg) plots of human glutathione S-transferases (GST) for the simulation of 20 ns with CPF, chlorpyrifos; CYPO, chlorpyrifosoxon; DEC, des-ethyl chlorpyrifos; TCP, 3,5,6- trichloro-2-pyridinol; TMP, 3,5,6-trichloro-2- methoxypyridine.

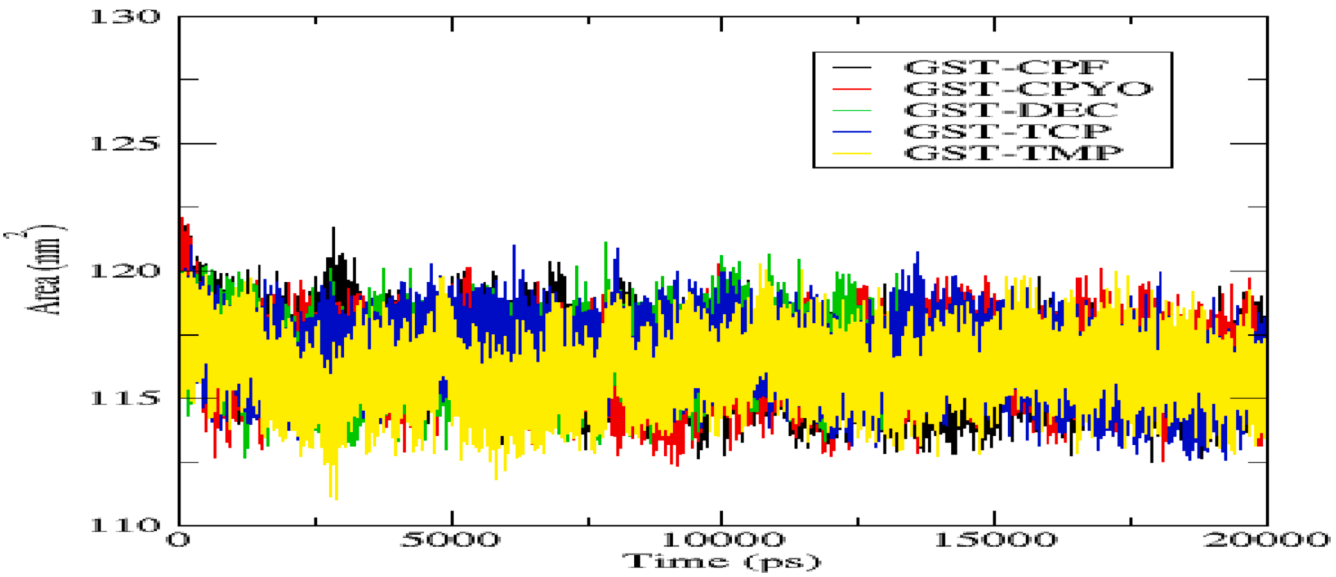

Fig. 9. Solvent accessible surface area profile of human glutathione S-transferases (GST) with CPF, CPYO, DEC,TCP and TMP during the simulation of 20 ns.

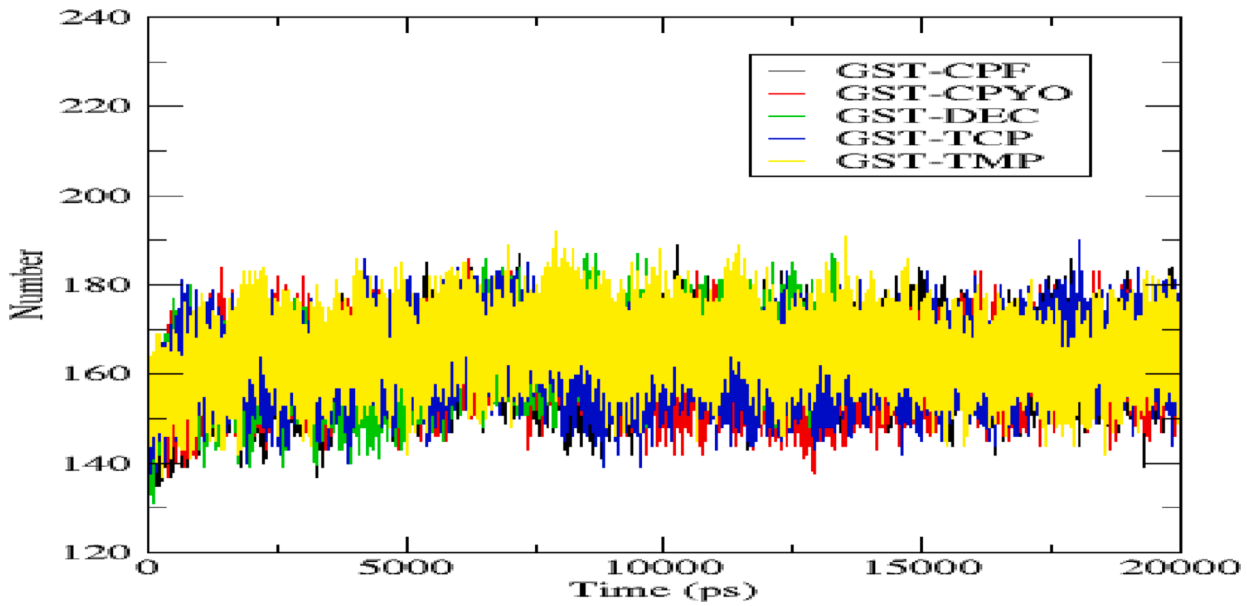

Fig. 10. Hydrogen bond number results of GST-CPF, GST-CPYO, GST-DEC, GST-TCP and GST-TMP complexes during the 20 ns of simulation.

RMSD results analysis implies that CPF and its degradants binding at the catalytic site of GST is stable and does not vary the protein stability.

Root mean square fluctuation, i.e., RMSF determines the fluctuation of Cα atom coordinates from their average position in the course of MD simulation. In the present context, atom mobility was calculated for all five GST-organophosphate ligand complexes and was plotted against the atom dependent on the trajectory of simulation, shown in Fig. 7. The results concluded that the active site residues were not much perturbed upon binding of the organophosphates. Results illustrate that the RMSF fluctuation profiles of GST-degradants of CPF complexes were almost similar to GST-CPF complex. Thus, the investigated organophosphates form stable complexes with GST and can inhibit this important enzyme.

Radius of gyration, i.e., Rg, it is a factor that can easily depict the protein compactness during molecular simulation. In general, lower value of Rg directly relate to dynamic stability of the investigated protein. In this current research work, the graph is plotted for Rg value against time as illustrated in Fig. 8. The results suggest that compactness for all of the five protein–ligand complexes is near about same.

Surface area that the probe of the solvent molecule monitors is solvent accessible surface area, i.e., SASA. Generally, alterations in structures are observed in the residues that form the loop region close to an active site cavity. Hydrophobic residues mostly give contribution in the rise of SASA value. SASA results of GST-degradants of CPF complexes are similar to GST-CPF complex as depicted in Fig. 9.

The stable conformation of protein directly depends on hydrogen bond interaction pattern. Hydrogen bond trajectory analysis for all the five complexes with respect to time was evaluated to understand the connection between flexibility and hydrogen bond formation. All the five investigated complexes showed comparable hydrogen bonds formation throughout the complete simulation of 20 ns (Fig. 10). For hydrogen bonds calculation, GROMACS utility, i.e., g hbond was employed. The hydrogen bond result enables one to understand the capability of such toxic organophosphates to efficiently inhibit the activite site of glutathione S-transferases (GST).

4. Conclusion

In this investigation, the inherent stability and biochemical interaction of chlorpyrifos and its degradants with human glutathione S-transferases (GST) as target have been studied using DFT and docking calculations and simulation. From, DFT calculation all the compounds are thermally stable and some of them show better chemical reactivity than chlorpyrifos. TCP show greater dipole moment with smaller HOMO-LUMO gap. Apart from that, TCP-GST complex shows better binding affinity with significant interactions than others. The docking results show that the hydrogen bonds, hydrophobic interactions, and binding energy of the compounds show the best binding capabilities when docked with human glutathione S-transferases (GST). In the comparison of these organophosphorus compounds, the binding affinity of TCP is −5.51 kcal/mol with the GST protein being the best binding energy among all the compounds. The compounds showed best binding energy, hydrophobic and hydrogen interactions to stabilize the protein–ligand complex.

Declaration of Competing Interest

The authors declare that they have no known competing financial interests or personal relationships that could have appeared to influence the work reported in this paper.

Data availability

No data was used for the research described in the article.

Acknowledgement

The authors are thankful to the head, Department of Chemistry, SRMCEM and to the Central Facility for Computational Research (CFCR), University of Lucknow for providing access to computational models throughout the work.

Funding

The authors declare that no funds, grants, or other support were received during the preparation of this manuscript.

References

[1] L.G. Sultatos, Mammalian toxicology of organophosphorus pesticides, J. Toxicol. Environ. Health 43 (1994) 271–289.
[2] T.R. Fukuto, Mechanism of action of organophosphorus and carbamate insecticides, Environ. Health Perspect. 87 (1990) 245–254.
[3] N. Zidan, A. El-Huda, Evaluation of the reproductive toxicity of chlorpyriphos methyl, diazinon and profenophos pesticides in male rats, Int. J. Pharmacol. 5 (2009) 51–57.
[4] K.D. Racke, Environmental fate of chlorpyrifos, Rev. Environ. Contam. Toxicol. 131 (1993) 1–151.
[5] L.G. Sultatos, L.D. Minor, S.D. Murphy, Metabolic activation of phosphorothionate pesticides: role of the liver, J. Pharmacol. Exp. Ther. 232 (1985) 624–628.
[6] M. Jokanovic, Biotransformation of organophosphorus compounds, Toxicology 166 (2001) 139–160.
[7] K. Fujioka, J.E. Casida, Glutathione S-transferase conjugation of organophosphorus pesticides yields S-phospho-, S-aryl-, and S-alkylglutathione derivatives, Chem. Res. Toxicol. 20 (2007) 1211–1217.
[8] S.K.M. Habeeb, V. Anuradha, A. Parveena, Comparative molecular modeling of insect glutathione S-transferases, Int. J. Comput. Appl. 14 (2011) 16–22.
[9] C.J. Whitten, D.L. Bull, Comparative toxicity, absorption and metabolism of chlorpyrifos and dimethyl homologue in methyl parathion-resistant and susceptible tobacco budworm, Pesticide Biochem. Physiol. 4 (1974) 266–274.
[10] B. Mannervik, U.H. Danielson, Glutathion transferases - structure and catalytic activity, CRC Crit. Rev. Biochem. 23 (1988) 283–337.
[11] A.S. Johansson, B. Mannervik, Human glutathione transferase A3–3, a highly efficient catalyst of double bond isomerization in the biosynthetic pathway of steroid hormones, J. Biol. Chem. 276 (2001) 32061–32065.
[12] M.M. Bhargava, I. Listowsky, I.M. Arias, Ligand in bilirubin binding and glutathione S-transferase activity is independent processes, J. Biol. Chem. 253 (1978) 4112–4115.
[13] T. Nikita, P. Anjali, K. Ashutosh, M. Anil, Computational investigation of dioxin-like compounds as human sex hormone-binding globulin inhibitors: DFT calculations, docking study and molecular dynamics simulations, Comput. Toxicol. 21 (2022), 100198.
[14] P. Townsend, M.N. Grayson, Density functional theory in the prediction of mutagenicity: a perspective, Chem. Res. Toxicol. 34 (2021) 179–188.
[15] R.G. Parr, Annu. Rev. Phys. Chem. 34 (1983) 631.
[16] R. Parthasarathi, J. Padmanabhan, V. Subramanian, B. Maiti, P.K. Chattaraj, J. Phys. Chem. A 107 (2003) 10346.
[17] R. Parthasarathi, J. Padmanabhan, V. Subramanian, U. Sarkar, B. Maiti, P. K. Chattaraj, Int. Electron. J. Mol. Des. 2 (2003) 798.
[18] J. Wan, L. Zhang, G.F. Yang, Quantitative structure-activity relationship for phenyl triazolinones of protoporphyrinogen oxidase inhibitors: a density functional theory study, J. Comput. Chem. 25 (2004) 1827–1832.
[19] A. Chakraborty, S. Giri, S. Duley, A. Anoop, P. Bultinck, P.K. Chattaraj, Aromaticity in all-metal annular systems: the counter-ion effect, Phys. Chem. Chem. Phys. 13 (2011) 14865–14878.
[20] L. Kuhnke, A. Ter Laak, A.H. Göller, Mechanistic reactivity descriptors for the prediction of ames mutagenicity of primary aromatic amines, J. Chem. Inf. Model 59 (2019) 668–672.
[21] J. Martínez, et al., Computational studies of Aflatoxin B1 (AFB1): a review, Toxins 15 (2023) 135.
[22] T. Nikita, P. Anjali, K. Ashutosh, M. Anil, Computational models reveal the potential of polycyclic aromatic hydrocarbons to inhibit aromatase, an important enzyme of the steroid biosynthesis pathway, Comput. Toxicol. 19 (2021), 100176.
[23] M.J. Frisch, et al., Gaussian 09, Revision D.01, Gaussian, Inc., Wallingford, CT, 2009.
[24] R. Dennington, T. Keith, J. Millam, GaussView, version 5, Semichem Inc., Shawnee Mission, KS, USA, 2009.
[25] A. Kumar, A. Mishra, Computational design, spectral, NBO, DOS, bioactivity evaluation, ADMET analysis, third-order nonlinear optical and quantum chemical investigations on hydrogen bonded novel organic molecular complex of 4-[Bis [2-(Acetyloxy) Ethyl] Amino] benzaldehyde (4B2AEAB) derivatives for Opto-electronic applications, Asian J. Chem. 32 (2020) 2793–2820.
[26] N. Tiwari, A. Mishra, C. Models, A sustainable approach to reveal the inhibitory potential of benzo(a)anthracene and its monohydroxy derivatives against human sex hormone-binding globulin, Indian J. Adv. Chem. Sci. 9 (2021) 250–254.
[27] D.R. Roy, E.V. Shah, S.M. Roy, Optical activity of Co-porphyrin in the light of IR and Raman spectroscopy: a critical DFT investigation, Spectrochimica Acta Part A: Mol. Biomol. Spectrosc. 190 (2018) 121–128.
[28] R.G. Pearson, The HSAB Principle-more quantitative aspects, Inorganica Chimica Acta 240 (1995) 93–98.
[29] Y.V. Patskovsky, L.N. Patskovska, I. Listowsky, An asparagine-phenylalanine substitution accounts for catalytic differences between hGSTM3-3 and other human class mu glutathione S-transferases, Biochemistry 38 (1999) 16187–16194.
[30] G.M. Morris, R. Huey, W. Lindstrom, M.F. Sanner, R.K. Belew, D.S. Goodsell, A. J. Olson, AutoDock4 and AutoDockTools4. Automated docking with selective receptor flexibility, J. Comput. Chem. 30 (2009) 2785–2791.
[31] W.L. DeLano, The PyMOL Molecular Graphics System, 2002.
[32] D. Van Der Spoel, E. Lindahl, B. Hess, G. Groenhof, A.E. Mark, H.J. Berendsen, GROMACS: fast, flexible, and free, J. Comput. Chem. 26 (2005) 1701–1718.
[33] W.F. van Gunsteren, S.R. Billeter, A.A. Eising, P.H. Hünenberger, P. Krüger, A.E. Mark, W.R. Scott, I.G. Tironi, Biomolecular Simulation: the {GROMOS96} Manual and User Guide, 1996.
[34] N. Balcı, H. Şakiroğlu, F. Türkan, E. Bursal, In vitro and in silico enzyme inhibition effects of some metal ions and compounds on glutathione S-transferase enzyme purified from Vaccinium arctostapylous L, J. Biomol. Struct. Dyn. 40 (2022) 11587–11593.